Toward a Smart Actuating System for Service Robots

TARIK UZUNOVIĆ [1] **(Senior Member, IEEE), ERAY A. BARAN** [2], **İLKAY TURAÇ ÖZÇELIK** [3],
MINORU YOKOYAMA [4] **(Member, IEEE), TOMOYUKI SHIMONO** [5] **(Senior Member, IEEE),**
AND ASIF ŠABANOVIĆ [6,7] **(Life Senior Member, IEEE)**

[1]Department of Automatic Control and Electronics, Faculty of Electrical Engineering, University of Sarajevo, 71000 Sarajevo, Bosnia and Herzegovina
[2]Department of Mechatronics Engineering, Faculty of Engineering and Natural Sciences, Istanbul Bilgi University, 34060 Istanbul, Turkey
[3]Department of Electrical and Electronics Engineering, Faculty of Engineering and Natural Sciences, Istanbul Bilgi University, 34060 Istanbul, Turkey
[4]Tokyu Construction Company, Ltd., Kanagawa 252-0244, Japan
[5]Faculty of Engineering, Yokohama National University, Yokohama 240-8501, Japan
[6]Faculty of Engineering and Natural Sciences, International University of Sarajevo, 71210 Ilidža, Bosnia and Herzegovina
[7]Academy of Sciences and Arts of Bosnia and Herzegovina, 71000 Sarajevo, Bosnia and Herzegovina

CORRESPONDING AUTHOR: TARIK UZUNOVIĆ (e-mail: tuzunovic@etf.unsa.ba).

ABSTRACT Owing to the increasing engagement of service robots in everyday life, significant requirements are imposed on their control systems to ensure safe interaction between robots and humans. The stiffness of the motion executed by the service robots is not high, as with industrial robots, but has to be variable depending on the defined task. Therefore, a service robot needs to have soft actuation, delivering "human-like" motion dependant on the interaction force between the robot and its environment. Such an operation requires switching from the trajectory tracking (position control) mode to the interaction (force control) mode, and *vice versa*. Conventional control methods, based on hybrid position/force control, or switching between a position and force controller, may fail short in these cases. Thus, we have previously proposed a new control method, denoted as universal motion controller, that merges the position and force control into a single control structure. The control method is elaborated in this article, and its experimental validation is presented for the first time for multi-degree-of-freedom systems.

INDEX TERMS Position/force control, robust control, service robots, universal motion controller.

I. INTRODUCTION

The world is facing a new era that is expected to bring more robots into our daily lives. The robots are nowadays not used only in industrial facilities, as the field of service robotics is having fast progress. When you mention the term "robot" today, one rarely thinks of an industrial manipulator trapped in a cage and operating in a structured and controlled environment. You would rather think of a robot helping industrial workers, serving food and drinks to customers in a restaurant, assisting or performing autonomously a medical surgery, or helping elderly people in their daily activities.

It is expected that in the near future, robots will revolutionize service industry by replacing human labor or having robots operating together with humans [1], [2]. It is also expected that complex tasks will be automated in manufacturing by the application of collaborative robotics [3]. The application of collaborative robots in a manufacturing process can improve not only production time but also ergonomics of the process [4]. Researchers are even considering proactive human–robot collaboration in industry [5]. The discussion of human–robot interaction takes into account even emotion recognition [6]. Successful collaboration between a robot and humans requires adaptive behavior and learning from the robot [7], as well as the capture of specific human skills [8].

Motion control is identified as one of the enabling technologies for successful cohabitation between humans and robots. Most human–robot collaborations require a smooth transition between the trajectory tracking (position) and interaction force control tasks [9], which are considered two basic tasks in

the motion control field [10]. Complex tasks can be described as a combination of the basic tasks. Thus, it is of essential importance to enable efficient position and force control, as well as to enable the transition between these two control modes. One has to note that trajectory tracking and force control tasks differ significantly in motion stiffness [11]; the control algorithm needs to enforce infinite stiffness for the position control mode, while on the contrary, the stiffness should be zero in the force control mode. Thus, the position and force control cannot be performed simultaneously along a single axis. One has to note that for multi-degree-of-freedom (multi-DOF) systems, it is possible to have position control along certain axes and force control along others, which yields the well-known hybrid control [12]. When a robot operates in a dynamic environment, position and force tracking may have to be used alternately along an axis, and the switching between the two control modes needs to be performed. Basic switching between position and force controllers is not a good resolution for several reasons. First, the switching between position and force control modes should be executed once the contact between the robot and its environment is established/lost, so the contact detection is imperative [13]. Second, switching between two different controllers may provoke highly oscillatory or, in the worst case, unstable behavior. We have tried to solve the stated problems by proposing a single control structure capable of controlling both position and force for a single-DOF system [14], and this was later generalized to multi-DOF systems [15]. Based on these findings, a new control system entitled universal motion controller was proposed [16]. The universal motion controller combines the position and force control to a single control structure, able to impose trajectory tracking in free motion and tracking of a reference force during contact with an environment. The transition between two control modes (position and force) is executed automatically. The universal motion controller can be applied for tasks specified in both the configuration and task spaces. The application of this control strategy for enabling soft actuation that can be applied to bilateral control and haptic reproduction is given in [17]. We discussed the construction of a smart actuating system based on the universal motion controller in [18]. In this article, we want to again underline the importance of the universal motion controller, further specify its potential for building a smart actuating system, and present first experimental results for this controller. In [15], we discussed multi-DOF position/force control only in the task space, while Uzunovic and Sabanovic [16] presented the possibility of single control structure for position/force control in both the configuration and task spaces, but without discussing a smart actuating system. Neither of these papers contained experimental results, and they are for the first time given in this article. Moreover, this article has given, in detail, the derivation of the attraction force dynamics necessary for the derivation of the control algorithm.

The rest of this article is organized as follows. Section II describes the algorithm of the universal motion controller and discusses the application of the universal motion controller in

a smart actuating system. Section III presents experimental results for a smart actuating system. Finally, Section IV concludes this article.

II. ALGORITHM OF THE UNIVERSAL MOTION CONTROLLER

The algorithm of the universal motion controller is presented in the first section. First, we will discuss the basic idea of the algorithm, and then, the model and disturbance compensation for the controlled system will be presented, while the mathematical formulation of the algorithm will later be given.

A. BASIC IDEA OF THE ALGORITHM

Let us assume that a robot is operating in an unstructured environment, and it is required to track a reference trajectory. In the free motion, the robot is controlled to enforce its convergence to the reference trajectory. However, during its motion, the robot may come into contact with an obstacle (human or some passive object) in the environment. Once the contact is established, the robot needs to be controlled to maintain the contact force at a desired level. The desired level may be the reference force or even the maximum allowed force. The maximum value may be selected to ensure safe operation and to avoid injury to humans in the environment or damage to the robot. Looking from the control point of view, during the free motion, the robot's position should be enforced to converge to the reference trajectory; during the contact, the robot's position should be modified to track the reference as much as possible, while keeping the contact force at the desired level. It means that the tracking of the reference may be possible in certain directions but impossible in the direction of the contact force. Thus, the control (input) force for the robot in the free motion is selected based on the discrepancy between its current and reference position. On the other hand, during the contact, the robot is required to modify its trajectory based on the current and reference interaction force. One needs to find a way to make the input force a function of the position and its reference in the free motion, but a function of the position, force, and their references during the contact. That is the basic idea of the universal motion controller's algorithm.

B. MODEL AND DISTURBANCE COMPENSATION

The controlled mechanical system will be denoted as a robot in the subsequent derivation. The robot is assumed to be a fully actuated mechanical system with n DOFs. The dynamics of the robot in the configuration space is described by [10]

$$\mathbf{A}(\mathbf{q})\ddot{\mathbf{q}} + \mathbf{b}(\mathbf{q}, \dot{\mathbf{q}}) + \mathbf{g}(\mathbf{q}) + \mathbf{T}_e = \mathbf{T} \qquad (1)$$

where $[q_1\, q_2 \ldots q_n]^{\mathrm{T}} = \mathbf{q} \in \mathbb{R}^{n \times 1}$ is the n-dimensional configuration vector; $\mathbf{A}(\mathbf{q}) \in \mathbb{R}^{n \times n}$ is the symmetric positive-definite inertia matrix of the robot; $\mathbf{b}(\mathbf{q}, \dot{\mathbf{q}}) \in \mathbb{R}^{n \times 1}$ stands for the Coriolis forces, viscous friction forces, and centripetal forces; $\mathbf{g}(\mathbf{q}) \in \mathbb{R}^{n \times 1}$ represents the vector of gravity forces; $\mathbf{T}_e \in \mathbb{R}^{n \times 1}$ models other external forces acting on the robot;

and $\mathbf{T} \in \mathbb{R}^{n \times 1}$ is the input force (i.e., control) vector. $\mathbf{T}_e$ represents the interaction forces that appear due to contact with the environment.

In many scenarios, the exact value of the inertia matrix is either difficult to calculate or even unknown beyond certain accuracy due to machining intolerances. Therefore, without loss of generality, one may assume the inertia as the sum of its nominal value $\mathbf{A}_n(\mathbf{q})$, which is assumed to be known, and the unknown variation $\Delta \mathbf{A}(\mathbf{q})$, as $\mathbf{A}(\mathbf{q}) = \mathbf{A}_n(\mathbf{q}) + \Delta \mathbf{A}(\mathbf{q})$. Typically, forces $\mathbf{b}(\mathbf{q}, \dot{\mathbf{q}}), \mathbf{g}(\mathbf{q})$, and $\mathbf{T}_e$ are difficult to model or measure; later, they are assumed to be unknown. Hence, one can rewrite the dynamics (1) in the following alternative form:

$$\mathbf{A}_n \ddot{\mathbf{q}} = \mathbf{T} - \mathbf{T}^{\mathrm{dis}}, \ \mathbf{T}^{\mathrm{dis}} = \mathbf{b} + \mathbf{g} + \mathbf{T}_e + \Delta \mathbf{A} \ddot{\mathbf{q}}. \quad (2)$$

In (2), $\mathbf{T}^{\mathrm{dis}}$ stands for the total disturbance force in the configuration space. Here, the explicit dependence of $\mathbf{A}_n(\mathbf{q})$ on $\mathbf{q}$ is omitted for shorter writing. The omission of explicit dependence $(\mathbf{q})$ will also be made in the remaining text for simpler analysis.

Under the assumption that accurate information of the configuration space velocity $\dot{\mathbf{q}}$ is available (measured or estimated), $\mathbf{T}^{\mathrm{dis}}$ can be estimated using the classical first-order disturbance observer (DOB) [11], [19], [20], implemented as suggested in [10], but for multi-DOF systems as given in [21]

$$\dot{\mathbf{z}}_d = \mathbf{L}_d \mathbf{A}_n^{-1} \left(\mathbf{T} - \mathbf{z}_d + \mathbf{L}_d \dot{\mathbf{q}} \right)$$

$$\hat{\mathbf{T}}^{\mathrm{dis}} = \mathbf{z}_d - \mathbf{L}_d \dot{\mathbf{q}} \quad (3)$$

where $\mathbf{L}_d \in \mathbb{R}^{n \times n}$ is a constant diagonal matrix containing the gains of the DOB, while $\mathbf{T}^{\mathrm{dis}} + \mathbf{L}_d \dot{\mathbf{q}} = \mathbf{z}_d \in \mathbb{R}^{n \times 1}$ is the intermediate variable in the disturbance estimation.

The input force $\mathbf{T}$ can be given as

$$\mathbf{T} = \mathbf{A}_n \ddot{\mathbf{q}}^{\mathrm{des}} + \hat{\mathbf{T}}^{\mathrm{dis}} \quad (4)$$

where $\ddot{\mathbf{q}}^{\mathrm{des}}$ is the desired configuration space acceleration. The form (4) is a classic solution in the acceleration control framework [10]. The selection of the desired acceleration $\ddot{\mathbf{q}}^{\mathrm{des}}$ can be made based on the task to be executed. Substituting (4) into (2) gives

$$\mathbf{A}_n \ddot{\mathbf{q}} = \mathbf{A}_n \ddot{\mathbf{q}}^{\mathrm{des}} + \underbrace{\left(\hat{\mathbf{T}}^{\mathrm{dis}} - \mathbf{T}^{\mathrm{dis}} \right)}_{\epsilon_{\mathrm{dis}}} \quad (5)$$

which is equivalent to

$$\ddot{\mathbf{q}} = \ddot{\mathbf{q}}^{\mathrm{des}} + \mathbf{A}_n^{-1} \epsilon_{\mathrm{dis}}. \quad (6)$$

Here, ϵ_{dis} represents the error in disturbance estimation in the configuration space. Perfect disturbance estimation ensures $\|\epsilon_{\mathrm{dis}}\| \to 0$. Therefore, the selection of $\ddot{\mathbf{q}}^{\mathrm{des}}$ has to be made according to the given task, which modifies (6) to $\ddot{\mathbf{q}} = \ddot{\mathbf{q}}^{\mathrm{des}}$.
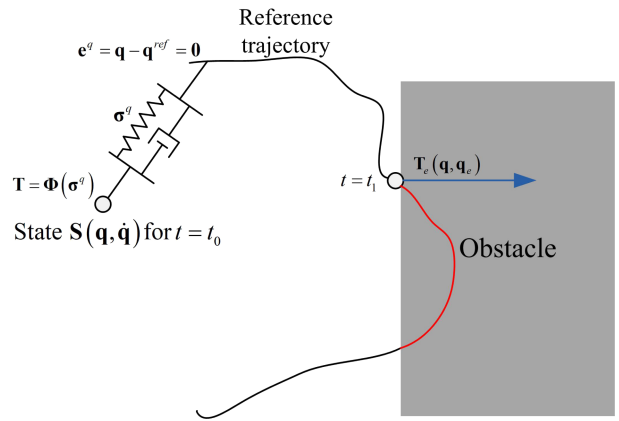

FIGURE 1. Basic idea of the algorithm.

C. UNIVERSAL MOTION CONTROLLER IN THE CONFIGURATION SPACE

It is assumed that the robot is required to track the reference $\mathbf{q}^{\mathrm{ref}}(t) \in \mathbb{R}^{n \times 1}$, which is a two times differentiable vector-valued function of time. During the contact motion, however, a nonzero interaction force $\mathbf{T}_e$ appears in the configuration space, which should be controlled to track a differentiable vector-valued reference force function of time $\mathbf{T}_e^{\mathrm{ref}}(t)$.

The position tracking error in the configuration space can be given as

$$\mathbf{e}^q = \mathbf{q} - \mathbf{q}^{\mathrm{ref}}. \quad (7)$$

Control input should then be selected to guarantee the convergence of the robot position $\mathbf{q}$ to the reference trajectory $\mathbf{q}^{\mathrm{ref}}$. In order to enforce the convergence, one can introduce the attraction force $\boldsymbol{\sigma}^q$ in the configuration space. The attraction force moves the current state of the robot to the desired state and attains a zero value if the robot is in the desired state. Since the robot can be moved only by the effect of $\mathbf{T}$, the input force $\mathbf{T}$ can then be expressed as a function of $\boldsymbol{\sigma}^q$. For trajectory tracking tasks, an apparent solution is to have $\boldsymbol{\sigma}^q = \mathbf{I} \dot{\mathbf{e}}^q + \mathbf{C}^q \mathbf{e}^q$, where $\mathbf{C}^q$ is a diagonal matrix with positive elements with $\mathbf{I}$ representing the identity matrix. It is assumed that entries of $\mathbf{I}$ and $\mathbf{C}^q$ have specific units, such that $\boldsymbol{\sigma}^q$ has the dimension of force in the configuration space. Therefore, for simplicity, the identity $\boldsymbol{\sigma}^q = \dot{\mathbf{e}}^q + \mathbf{C}^q \mathbf{e}^q$ will be used in the remaining text. This definition of the attraction force implies that the attraction between the reference $\mathbf{q}^{\mathrm{ref}}$ and the current $\mathbf{q}$ position is modeled with a spring–damper dynamics, as illustrated in Fig. 1. On the other hand, during an interaction with the environment $\boldsymbol{\sigma}^q$ should depend on the nonzero interaction force $\mathbf{T}_e$. The physical interpretation of this approach represents the modification of the robot's motion profile (red part of the reference in Fig. 1). Once the reference trajectory is modified, the magnitude of $\mathbf{e}^q$ increases. An uncontrolled increase of the interaction force $\boldsymbol{\sigma}^q$ has to be restricted, preventing an uncontrolled increase in the input force $\mathbf{T}$ and, thus, a potential damage on the robot or its environment. Yet, if the magnitude of $\boldsymbol{\sigma}^q$ depends on $\mathbf{T}_e$ and $\mathbf{T}_e^{\mathrm{ref}}$, it will be possible to

have a definition of the attraction force $\boldsymbol{\sigma}^q$ for both the position and force control tasks.

The interaction force in the configuration space can be modeled as

$$\mathbf{T}_e = \begin{cases} \mathbf{0}, & \text{no contact} \\ D_e\left(\dot{\mathbf{q}} - \dot{\mathbf{q}}_e\right) + K_e\left(\mathbf{q} - \mathbf{q}_e\right), & \text{in contact} \end{cases} \quad (8)$$

where $K_e = K_{\mathrm{en}} + \Delta K_e$ and $D_e = D_{\mathrm{en}} + \Delta D_e$ denote the stiffness and damping coefficients of the environment at the interaction point, respectively, while $\mathbf{q}_e = [q_{e1}\, q_{e2} \ldots q_{en}]^{\mathrm{T}}$ denotes the position of the environment. In the rest of the text, the term environment position will refer to the position of the contact point that belongs to an obstacle. The precise values of D_e and K_e are, in general, unknown. Hence, in (8), K_{en} and D_{en}, respectively, stand for the known nominal values of the stiffness and damping coefficients. On the other hand, the terms ΔK_e and ΔD_e represent the unknown variations around the assumed nominal values of the stiffness and damping, respectively. It is important to note that the identity (8) may result in positive and negative values for the constituents of the interaction force during the contact. The alternation of the sign denotes the alternation of the force direction. Thus, each component of the interaction force can have a positive reference $T_{ei+}^{\mathrm{ref}} > 0$ and a negative reference $T_{ei-}^{\mathrm{ref}} < 0$ ($i = 1, 2, \ldots, n$). Depending on the given task, the positive reference can coincide with the interaction force resulting from a positive i-direction motion, and a similarly negative reference may coincide with the interaction force with the opposite direction.

Here, one can define the necessary intermediate variable $\boldsymbol{\eta}^q$, which represents componentwise saturated attraction force defined for pure trajectory tracking tasks. The limits of $\boldsymbol{\eta}^q$ depend on the reference interaction force whose components are

$$\eta_i^q = \begin{cases} \dot{e}_i^q + c_i^q e_i^q, & \text{if } -\rho T_{ei+}^{\mathrm{ref}} < \dot{e}_i^q + c_i^q e_i^q < -\rho T_{ei-}^{\mathrm{ref}} \\ -\rho T_{ei-}^{\mathrm{ref}}, & \text{if } \dot{e}_i^q + c_i^q e_i^q \geq -\rho T_{ei-}^{\mathrm{ref}} \\ -\rho T_{ei+}^{\mathrm{ref}}, & \text{if } \dot{e}_i^q + c_i^q e_i^q \leq -\rho T_{ei+}^{\mathrm{ref}} \end{cases}. \quad (9)$$

In (9), e_i^q is the ith component of $\mathbf{e}^q$, $c_i^q > 0$ represents the entries of the diagonal matrix $\mathbf{C}^q$, and $\rho > 0$ is a constant.

Finally, the attraction force $\boldsymbol{\sigma}^q$ can be given as

$$\boldsymbol{\sigma}^q = \left[\sigma_1^q\, \sigma_2^q \ldots \sigma_n^q\right]^{\mathrm{T}} = \boldsymbol{\eta}^q + \rho \mathbf{T}_e. \quad (10)$$

During the implementation, the attraction force attains a zero value if the controlled system reaches the desired state. Consequently, the control algorithm is designed to enforce $\boldsymbol{\sigma}^q$ converge to zero [16].

The dynamics of the ith σ_i^q component of $\boldsymbol{\sigma}^q$ is given as follows:

$$\dot{\sigma}_i^q = \ddot{q}_i - \ddot{q}_i^{\mathrm{ref}} + c_i^q \dot{e}_i^q$$
$$+ \rho \dot{T}_{ei}, \quad \text{if } -\rho T_{ei+}^{\mathrm{ref}} < \dot{e}_i^q + c_i^q e_i^q < -\rho T_{ei-}^{\mathrm{ref}} \quad (11)$$

$$\dot{\sigma}_i^q = \rho D_e \ddot{q}_i - \rho D_e \ddot{q}_{ei}$$
$$+ \rho K_e(\dot{q}_i - \dot{q}_{ei}) - \rho \dot{T}_{ei-}^{\mathrm{ref}}, \quad \text{if } \dot{e}_i^q + c_i^q e_i^q \geq -\rho T_{ei-}^{\mathrm{ref}} \quad (12)$$

$$\dot{\sigma}_i^q = \rho D_e \ddot{q}_i - \rho D_e \ddot{q}_{ei}$$
$$+ \rho K_e(\dot{q}_i - \dot{q}_{ei}) - \rho \dot{T}_{ei+}^{\mathrm{ref}}, \quad \text{if } \dot{e}_i^q + c_i^q e_i^q \leq -\rho T_{ei+}^{\mathrm{ref}}. \quad (13)$$

A general form, considering each of these cases, would be

$$\dot{\sigma}_i^q = \alpha_i \left(\ddot{q}_i - \dot{\sigma}_i^d\right) \quad (14)$$

where α_i and $\dot{\sigma}_i^d$ are

$$\alpha_i = \begin{cases} 1, & \text{if } -\rho T_{ei+}^{\mathrm{ref}} < \dot{e}_i^q + c_i^q e_i^q < -\rho T_{ei-}^{\mathrm{ref}} \\ \rho D_e, & \text{if } \dot{e}_i^q + c_i^q e_i^q \geq -\rho T_{ei-}^{\mathrm{ref}} \\ \rho D_e, & \text{if } \dot{e}_i^q + c_i^q e_i^q \leq -\rho T_{ei+}^{\mathrm{ref}} \end{cases} \quad (15)$$

$$\dot{\sigma}_i^d = \ddot{q}_i^{\mathrm{ref}} - c_i^q \dot{e}_i^q - \rho \dot{T}_{ei}$$
$$\text{if } -\rho T_{ei+}^{\mathrm{ref}} < \dot{e}_i^q + c_i^q e_i^q < -\rho T_{ei-}^{\mathrm{ref}} \quad (16)$$

$$\dot{\sigma}_i^d = \ddot{q}_{ei} - K_e D_e^{-1}(\dot{q}_i - \dot{q}_{ei}) + D_e^{-1}\dot{T}_{ei-}^{\mathrm{ref}},$$
$$\text{if } \dot{e}_i^q + c_i^q e_i^q \geq -\rho T_{ei-}^{\mathrm{ref}} \quad (17)$$

$$\dot{\sigma}_i^d = \ddot{q}_{ei} - K_e D_e^{-1}(\dot{q}_i - \dot{q}_{ei}) + D_e^{-1}\dot{T}_{ei+}^{\mathrm{ref}}$$
$$\text{if } \dot{e}_i^q + c_i^q e_i^q \leq -\rho T_{ei+}^{\mathrm{ref}}. \quad (18)$$

In general, for the dynamics of $\boldsymbol{\sigma}^q$, one can write

$$\dot{\boldsymbol{\sigma}}^q = \boldsymbol{\alpha}\left[\ddot{\mathbf{q}} - \dot{\boldsymbol{\sigma}}^d\right]. \quad (19)$$

Considering (19), as well as (6), the dynamics of the attraction force can be written as

$$\dot{\boldsymbol{\sigma}}^q = \boldsymbol{\alpha}\left[\ddot{\mathbf{q}}^{\mathrm{des}} - \dot{\boldsymbol{\sigma}}^{\mathrm{dis}}\left(\mathbf{q}, \mathbf{q}^{\mathrm{ref}}, \mathbf{q}_e, \mathbf{T}_e, \mathbf{T}_e^{\mathrm{ref}}, \rho, \boldsymbol{\epsilon}_{\mathrm{dis}}\right)\right]. \quad (20)$$

The loop gain matrix $\boldsymbol{\alpha} = \mathrm{diag}(\alpha_1, \alpha_2, \ldots, \alpha_n)$ is a diagonal matrix whose ith element α_i modifies depending whether the related ith component η_i^q of $\boldsymbol{\eta}^q$ has reached its limit values or not. If η_i^q reaches $-\rho T_{ei-}^{\mathrm{ref}}$ or $-\rho T_{ei+}^{\mathrm{ref}}$, then $\alpha_i = \rho D_e$; otherwise, $\alpha_i = 1$. Assuming available nominal value for D_e, one can have the same dynamic model for (20) except that $\alpha_i = \rho D_{\mathrm{en}}$ when η_i^q reaches $-\rho T_{ei-}^{\mathrm{ref}}$ or $-\rho T_{ei+}^{\mathrm{ref}}$. For $\rho = D_{\mathrm{en}}^{-1}$, $\boldsymbol{\alpha}$ is an identity matrix. Here, it should be emphasized that the loop gain changes depending on $\boldsymbol{\eta}^q$; hence, the system may show oscillatory behavior if the control gains of the controller are not chosen properly. Generally, ρ should have a small value for hard contacts.

When $\boldsymbol{\sigma}^q$ is available, $\dot{\boldsymbol{\sigma}}^{\mathrm{dis}}$ can be estimated using the same approach as in (3)

$$\dot{\mathbf{z}}_\sigma = \mathbf{L}_\sigma \boldsymbol{\alpha}\left(\ddot{\mathbf{q}}^{\mathrm{des}} - \mathbf{z}_\sigma + \mathbf{L}_\sigma \boldsymbol{\sigma}^q\right)$$
$$\hat{\boldsymbol{\sigma}}^{\mathrm{dis}} = \mathbf{z}_\sigma - \mathbf{L}_\sigma \boldsymbol{\sigma}^q \quad (21)$$

where $\mathbf{L}_\sigma \in \mathbb{R}^{n \times n}$ represents the gain matrix of the observer given as a constant diagonal matrix, and $\dot{\boldsymbol{\sigma}}^{\mathrm{dis}} + \mathbf{L}_\sigma \boldsymbol{\sigma}^q = \mathbf{z}_\sigma \in \mathbb{R}^{n \times 1}$ stands for the intermediate variable in the estimation.

When $\hat{\boldsymbol{\sigma}}^{\mathrm{dis}}$ is available, one can select $\ddot{\mathbf{q}}^{\mathrm{des}}$ as

$$\ddot{\mathbf{q}}^{\mathrm{des}} = \hat{\boldsymbol{\sigma}}^{\mathrm{dis}} - \boldsymbol{\alpha}^{-1}\boldsymbol{\Psi}(\boldsymbol{\sigma}^q) \quad (22)$$

where

$$\dot{\sigma}^q + \Psi(\sigma^q) = \mathbf{0} \qquad (23)$$

defines the desired first-order dynamics of σ^q. The possible solutions are as follows.

1) For exponential convergence, one should select

$$\Psi(\sigma^q) = \mathbf{K}\sigma^q \qquad (24)$$

where $\mathbf{K}$ is a constant diagonal matrix with positive entries.

2) For finite-time convergence

$$\Psi(\sigma^q) = \mathbf{K} \begin{bmatrix} \left(\text{abs}\left(\sigma_1^q\right)\right)^\beta \text{sign}\left(\sigma_1^q\right) \\ \left(\text{abs}\left(\sigma_2^q\right)\right)^\beta \text{sign}\left(\sigma_2^q\right) \\ \vdots \\ \left(\text{abs}\left(\sigma_n^q\right)\right)^\beta \text{sign}\left(\sigma_n^q\right) \end{bmatrix}, \quad 0 \le \beta < 1 \qquad (25)$$

where $\beta = 0$ enforces the sliding-mode control and $0 < \beta < 1$ provides a finite-time convergence with continuous control signal.

D. UNIVERSAL MOTION CONTROLLER IN THE TASK SPACE

In a wide range of applications, the desired operations of the robot are defined in the task space. The execution of the goals may require the task space position $\mathbf{x}(\mathbf{q}) \in \mathbb{R}^{m \times 1}$ to track the reference trajectory $\mathbf{x}^{\text{ref}}(t) \in \mathbb{R}^{m \times 1}$. The interaction force in the task space $\mathbf{F}_e \in \mathbb{R}^{m \times 1}$, on the other hand, should be controlled to track its reference $\mathbf{F}_e^{\text{ref}} \in \mathbb{R}^{m \times 1}$ in the contact motion.

The design procedure of the controller depends on the calculation of the attraction force σ^x in the task space. The task space position tracking error can be given as

$$\mathbf{e}^x = \mathbf{x} - \mathbf{x}^{\text{ref}}. \qquad (26)$$

The intermediate variable η^x with the components ($i = 1, 2, \ldots, m$) can then be calculated using the following formulation:

$$\eta_i^x = \begin{cases} \dot{e}_i^x + c_i^x e_i^x, & \text{if } -\rho F_{e i-}^{\text{ref}} < \dot{e}_i^x + c_i^x e_i^x < -\rho F_{e i-}^{\text{ref}} \\ -\rho F_{e i-}^{\text{ref}}, & \text{if } \dot{e}_i^x + c_i^x e_i^x \ge -\rho F_{e i-}^{\text{ref}} \\ -\rho F_{e i+}^{\text{ref}}, & \text{if } \dot{e}_i^x + c_i^x e_i^x \le -\rho F_{e i+}^{\text{ref}} \end{cases} \qquad (27)$$

where e_i^x represents the ith component of the vector $\mathbf{e}^x$, c_i^x stands for the positive diagonal entries of the diagonal matrix $\mathbf{C}^x$, and ρ is a positive constant. The attraction force σ^x is then given by

$$\sigma^x = \begin{bmatrix} \sigma_1^x \sigma_2^x \ldots \sigma_m^x \end{bmatrix}^T = \eta^x + \rho \mathbf{F}_e. \qquad (28)$$

The calculated forces can be transformed from the task space to the configuration space using the transposed Jacobian matrix $\mathbf{J}^T$, where $\mathbf{J} = \frac{\partial \mathbf{x}}{\partial \mathbf{q}} \in \mathbb{R}^{m \times n}$. Hence, the attraction force for the configuration space can be calculated from

$$\sigma^q = \mathbf{J}^T \sigma^x. \qquad (29)$$

Once σ^q is obtained, the rest of the control design procedure can be handled similar to the configuration space calculations as explained in the previous section.

It is important to highlight here that the universal motion control algorithm is based on the attraction force σ^q. Assuming a task being defined directly in the configuration space, calculation of σ^q can be directly made using the measured and reference variables. On the other hand, the tasks defined directly in the task space require the calculation of the attraction force in the task space (i.e., σ^x), which can then be transformed to the joint space attraction force using the transposed Jacobian. In other words, the universal motion control algorithm always required the attraction force σ^q, which is defined in the configuration space. It is not of a great importance for the controller's performance whether the attraction force is directly obtained from the configuration space variables or obtained from the task space variables and mapped to configuration space with proper transformations.

The smart actuation scheme detailed in this article refers to a system, which can be used in a plug-and-play form for an arbitrary manipulator with proper sensor interface. The control system designer needs to provide the necessary position and force references and define the proper transformations between the configuration and task spaces. More specifically, the transposed Jacobian $\mathbf{J}^T$ is necessary for mapping the task space attraction force σ^x to the configuration space attraction force σ^q.

Fig. 2 shows a depiction of the smart actuating system functional for the task space control; however, even a simpler structure can be depicted for the configuration space control. As also shown in that figure, the control system designer needs to provide trajectory reference $\mathbf{x}^{\text{ref}}$ and force reference defined by $\mathbf{F}_{e-}^{\text{ref}} = [F_{e 1-}^{\text{ref}} \ldots F_{e m-}^{\text{ref}}]^T$ and $\mathbf{F}_{e+}^{\text{ref}} = [F_{e 1+}^{\text{ref}} \ldots F_{e m+}^{\text{ref}}]^T$. Moreover, the transformation of positions/velocities and forces from the configuration space to the task space has to be defined, from which one can obtain the transposed Jacobian.

Besides the transformations, the designer has to define several control parameters: $\mathbf{A}_n$, nominal inertia matrix; $\mathbf{L}_d$, gain matrix for the configuration space disturbance estimation; $\mathbf{L}_\sigma$, gain matrix for the estimation of $\dot{\sigma}^{\text{dis}}$; $\mathbf{C}^x$, for η^x calculation; ρ, for σ^x calculation; and D_{en}, nominal value of the damping coefficient of the environment. It is important to note that nominal inertia matrix can be evaluated using some of the identification approaches. One of them, offering a real-time identification approach, is given in [22]. Provided with these parameters, the smart actuating system will be capable of enforcing the tracking of the free motion position and the contact motion force references in a unified structure.

III. EXPERIMENTAL VALIDATION
A. EXPERIMENTAL SETUP

The proposed algorithm is validated on an experimental setup consisted of a pantograph robot mechanism and several obstacles with different geometries acting as the environment.
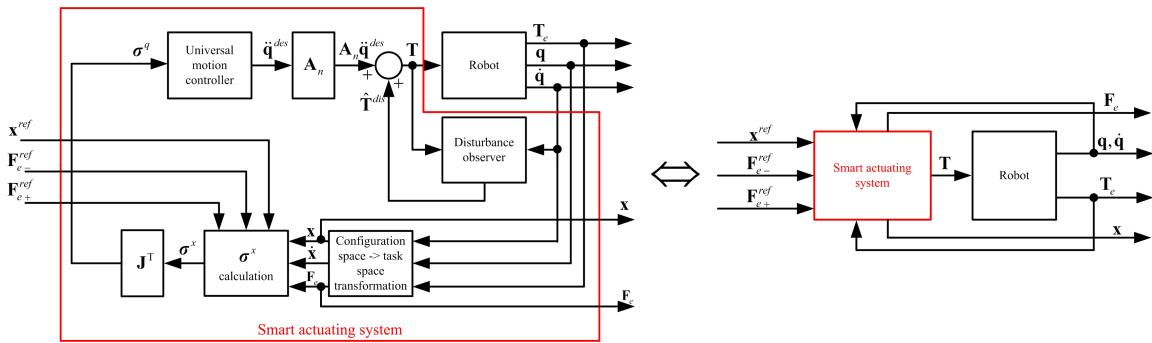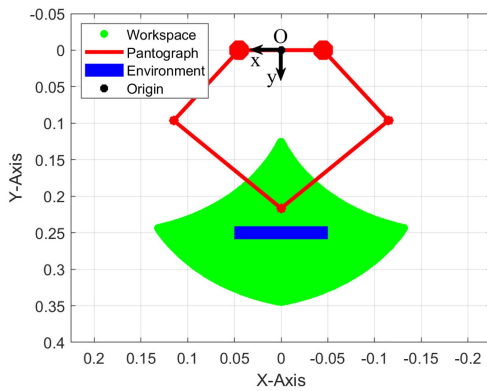
FIGURE 2. Smart actuating system.

FIGURE 3. Dimensions, axes assignment, and workspace illustration of the pantograph robot.

FIGURE 4. Photo of the experimental setup.

The robot contains two brushless dc motors from Faulhaber 3242G012-BX4 series. The motors have integrated incremental quadrature encoders with 10 000 lines/rev resolution and backdrivable zero-backlash gearboxes with a reduction ratio of 1:19. Combined with the gearboxes, the resolution of the motion at the output shaft of these actuators becomes $0.000473°$. The motors are powered by two Faulhaber MCBL-3006S series drivers, which are configured for operation in the current control mode. The dimensions and the workspace of the robot, the relative position of the environment, and the assignment of the axes are illustrated in the drawing given in Fig. 3. The implementation of the proposed algorithm is made using C coding on a real-time programmable logic controller (PLC) system from B&R 1586 series . The code is executed with a sampling period of 200 μs (i.e., with a loop frequency of 5 kHz). The estimation of the contact force is realized by the reaction force observer algorithm [23] after proper transformations using the transposed Jacobian of the corresponding kinematic chain. Referring to Fig. 3, the base length and the lengths of the arms are, respectively, measured as $h = 0.09$ m and $l_1 = 0.15$ m, $l_2 = 0.20$ m. For the sake of completeness, a photo of the experimental setup is also shown in Fig. 4 .
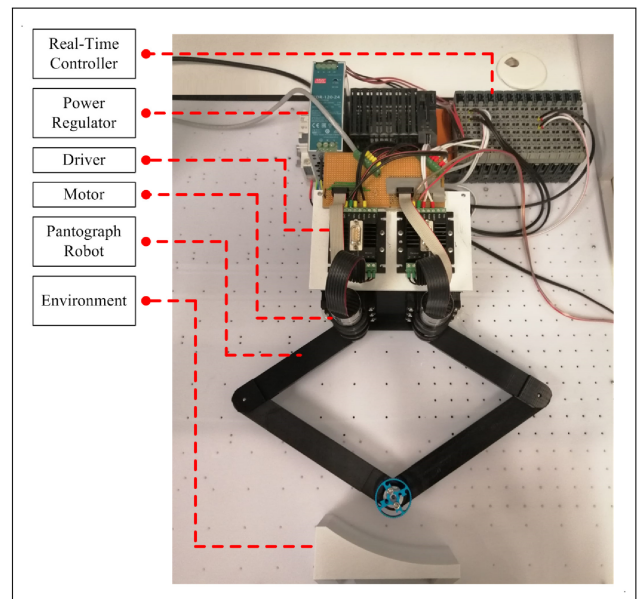
B. EXPERIMENTAL RESULTS

In order to better illustrate the performance of the proposed algorithm, the experimental validation is made using three different experiment configurations. In each configuration, different obstacle geometries and references for positions and forces are used. The details related to these configurations are as follows. In the first experiment (i.e., Exp-1), a flat environment geometry is chosen, and sinusoidal position and force references are preferred. This experiment specifically addresses the basic transitions between force and position control modes of the proposed algorithm. In the second experiment (denoted as Exp-2), a circular environment geometry is used. The reference position profile is selected such that the force control mode is triggered during continuous position tracking over the curved surface. The third experiment (i.e., Exp-3) is configured to contain a triangular edge profile in the environment. Here, the same position profile is preferred, while the force reference is increased to illustrate successful transition to force control right at the corner point of the environment. The values of the control parameters used in the
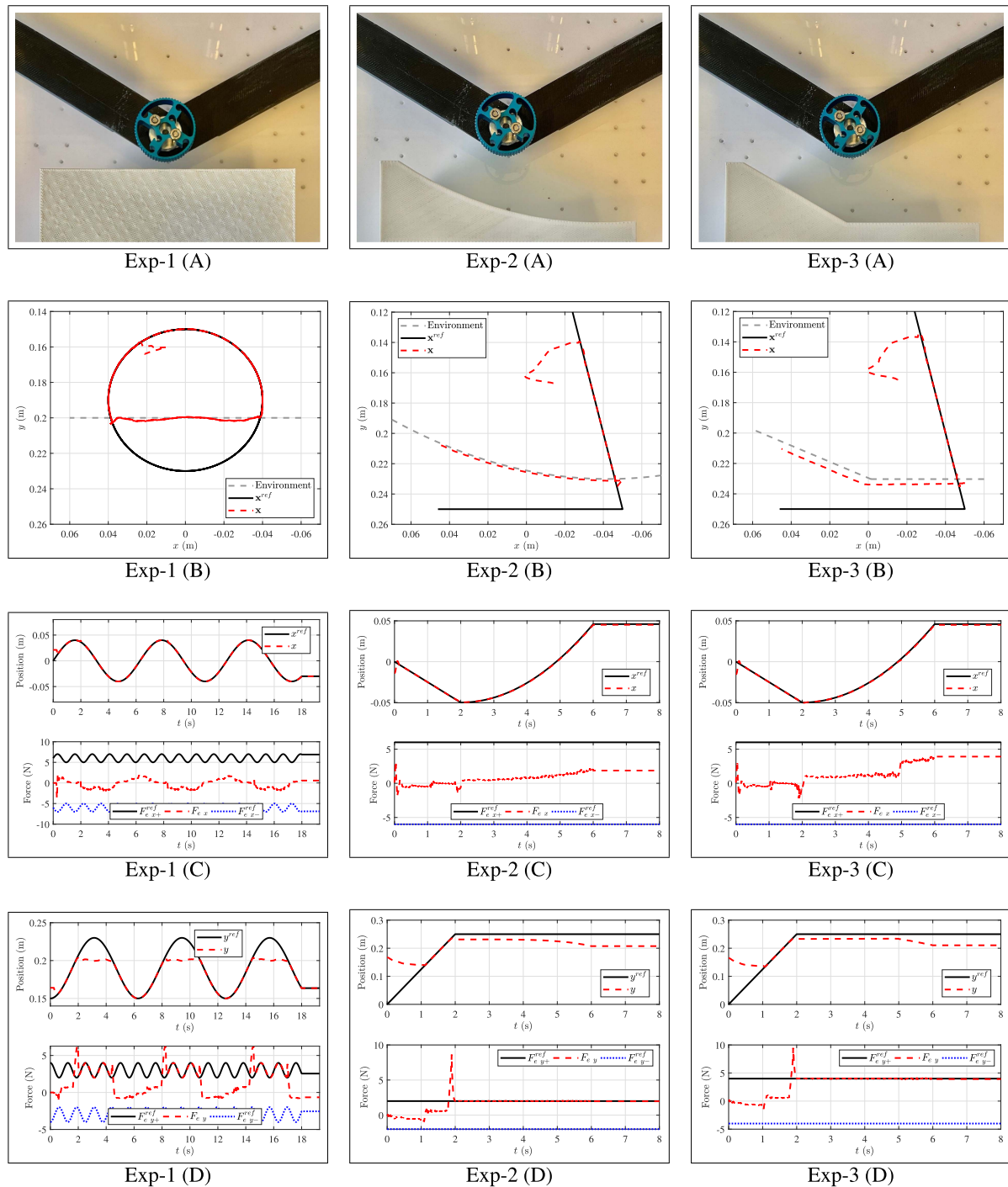
FIGURE 5. Experimental results with different environmental geometries. Row-1: Pictures of the experimental setup. Row-2: Cartesian position responses along with the obstacle positions. Row-3: *x*-direction position and interaction force responses. Row-4: *y*-direction position and interaction forces. The columns correspond to the experiments with flat (A), round (B), and inclined (C) geometries for the selected environment.

experimental validation are listed in Table 1. The controller gains are empirically tuned to catch the desired performance characteristics.

The results of the first experiment are given in Fig. 5. In that figure, the first row shows the pictures of the selected environment profiles. The second row illustrates the Cartesian position reference and responses for each experiment, whereas the third and fourth rows depict the position and force responses of the *x*-axis and the *y*-axis, respectively. Each column of Fig. 5 corresponds to one of the experiment configurations described above.

The responses shown in Exp-1 (B) show that the robot tracks the reference in the free motion. When it comes in contact with the environment, it is able to track its reference in

TABLE 1. Parameters Used in the Experiments

Parameter	Explanation	Value
K_{en}	Nominal stiffness coefficient	5000 N/m
D_{en}	Nominal damping coefficient	17 N·s/m
ρ	Constant	0.06
$\mathbf{C}^q$	Matrix used for $\boldsymbol{\eta}^q$ definition	$\mathrm{diag}(40, 40)$
$\mathbf{K}$	Controller gain	$\mathrm{diag}(8000, 5000)$
$\mathbf{L}_d$	Gain matrix for $\hat{\mathbf{T}}^{dis}$ estimation	$\mathrm{diag}(2500, 2500)$
$\mathbf{L}_\sigma$	Gain matrix for $\hat{\boldsymbol{\sigma}}^{dis}$ estimation	$\mathrm{diag}(2500, 2500)$

the x-direction [see Exp-1 (C)]. However, when the reference trajectory goes "behind" the environment (i.e., beyond the initial contact point along the axis of motion), the tracking is lost in the y-direction, the controller switches to the force control mode, and interaction force can now be controlled in this direction. Exp-1 (D) depicts successful force tracking in the y-direction during the contact motion. Overshoot in the force response during the establishment of the contact between the robot and environment is expected, and it is the impact force that appears during contact with a stiff environment. Nonzero measured force during the free motion is the consequence of the usage of reaction force observer. Since this article is not concerned with high precision force measurement, this kind of behavior is acceptable. Superior force measurement would provide much better force responses.

The results of the second experiment are provided in Fig. 5, Exp-2 (B) to Exp-2 (D). The environment had a curved shape in this experiment. The robot is able to track the reference in the free motion [see Exp-2 (B)]. When the robot establishes contact with the environment, the reference tracking is maintained in the x-direction [see Exp-2 (C)]. Nevertheless, when the reference trajectory goes "behind" the environment, the tracking is lost in the y-direction (around 1.8 s). The control algorithm automatically switches to the force control mode, and interaction force is controlled in this direction. Exp-2 (D) shows successful force tracking in the y-direction during the contact motion. Overshoot in the force response during the establishment of the contact between the robot and environment and nonzero measured force during the free motion appears again for the aforementioned reasons.

The results of the third experiment are provided in Fig. 5, Exp-3 (B) to Exp-3 (D). The environment shape was now changed with respect to the previous experiment. The robot converges to and tracks the reference trajectory in the free motion [see Exp-3 (B)]. When it comes into contact with the environment, the reference tracking is preserved in the x-direction [see Exp-3 (C)]. On the other hand, as the reference trajectory goes "behind" the environment, the tracking is lost in the y-direction. The control algorithm switches to the force control mode, and the interaction force is controlled in the y-direction. Exp-3 (D) shows successful force tracking in the y-direction during the contact motion. Overshoot in the force response during the establishment of the contact between the

robot and environment and nonzero measured force during the free motion appears for the aforementioned reasons.

IV. CONCLUSION

This article presented and validated a unified control strategy that enables the implementation of a smart actuating system for service robots. The control strategy realized the position and the force control modes using a single control structure, in both the configuration and task spaces. Switching between the free motion and contact motion modes was performed automatically, without the requirement for a specific algorithm to detect the contact with an object. The actuating system, enabled by the control algorithm, can be applied in a plug-and-play fashion for an arbitrary mechanical system (robot). The proposed algorithm required from the designer a few control parameters and measured and reference values, which makes it easy to tune and, hence, be directly applied for most of the motion control tasks demanded from service robots.

REFERENCES

[1] J. Wirtz et al., "Brave new world: Service robots in the frontline," *J. Service Manage.*, vol. 29, no. 5, pp. 907–931, 2018.

[2] J. Wirtz, W. Kunz, and S. Paluch, "The service revolution, intelligent automation and service robots," *Eur. Bus. Rev.*, vol. 29, pp. 38–44, 2021.

[3] D. Kragic, J. Gustafson, H. Karaoguz, P. Jensfelt, and R. Krug, "Interactive, collaborative robots: Challenges and opportunities," in *Proc. 27th Int. Joint Conf. Artif. Intell.*, 2018, pp. 18–25.

[4] M. Pearce, B. Mutlu, J. Shah, and R. Radwin, "Optimizing makespan and ergonomics in integrating collaborative robots into manufacturing processes," *IEEE Trans. Autom. Sci. Eng.*, vol. 15, no. 4, pp. 1772–1784, Oct. 2018.

[5] S. Li, P. Zheng, J. Fan, and L. Wang, "Towards proactive human robot collaborative assembly: A multimodal transfer learning-enabled action prediction approach," *IEEE Trans. Ind. Electron.*, vol. 69, no. 8, pp. 8579–8588, Aug. 2022.

[6] L. Chen, K. Wang, M. Li, M. Wu, W. Pedrycz, and K. Hirota, "K-means clustering-based kernel canonical correlation analysis for multimodal emotion recognition in human–robot interaction," *IEEE Trans. Ind. Electron.*, vol. 70, no. 1, pp. 1016–1024, Jan. 2023, doi: 10.1109/TIE.2022.3150097.

[7] X. Zhao, S. Han, B. Tao, Z.-P. Yin, and H. Ding, "Model-based actor-critic learning of robotic impedance control in complex interactive environment," *IEEE Trans. Ind. Electron.*, vol. 69, no. 12, pp. 13225–13235, Dec. 2022, doi: 10.1109/TIE.2021.3134082.

[8] H. Ochoa and R. Cortesão, "Impedance control architecture for robotic-assisted mold polishing based on human demonstration," *IEEE Trans. Ind. Electron.*, vol. 69, no. 4, pp. 3822–3830, Apr. 2022.

[9] G. Michalos et al., "Seamless human robot collaborative assembly—An automotive case study," *Mechatronics*, vol. 55, pp. 194–211, 2018, doi: 10.1016/j.mechatronics.2018.08.006.

[10] A. Šabanović and K. Ohnishi, *Motion Control Systems*. Singapore: Wiley, 2011.

[11] K. Ohnishi, M. Shibata, and T. Murakami, "Motion control for advanced mechatronics," *IEEE/ASME Trans. Mechatron.*, vol. 1, no. 1, pp. 56–67, Mar. 1996.

[12] O. Khatib, "A unified approach for motion and force control of robot manipulators: The operational space formulation," *IEEE J. Robot. Autom.*, vol. RA-3, no. 1, pp. 43–53, Feb. 1987.

[13] N. Shimada, K. Ohishi, T. Yoshioka, and T. Miyazaki, "Quick and reliable contact detection for sensorless force control of industrial robots for human support," in *Proc. IEEE Int. Symp. Ind. Electron.*, 2012, pp. 1674–1679.

[14] T. Uzunovic, A. Sabanovic, M. Yokoyama, and T. Shimono, "Novel algorithm for effective position/force control," *IEEJ J. Ind. Appl.*, vol. 8, no. 6, pp. 960–966, 2019.

[15] T. Uzunovic, A. Sabanovic, M. Yokoyama, and T. Shimono, "Novel algorithm for position/force control of multi-DOF robotic systems," in *Proc. IEEE 16th Int. Workshop Adv. Motion Control*, 2020, pp. 273–278.

[16] T. Uzunovic and A. Sabanovic, "Universal motion controller," in *Proc. IEEE 30th Int. Symp. Ind. Electron.*, 2021, pp. 1–6.

[17] A. Šabanović, T. Uzunović, E. A. Baran, M. Yokoyama, and T. Shimono, "Application of soft actuation to bilateral control and haptic reproduction," *Int. J. Control, Autom. Syst.*, vol. 20, no. 3, pp. 992–1001, 2022.

[18] T. Uzunović and A. Šabanović, "Merging position and force control into a single control structure: One step towards smart actuating system," in *Proc. IEEE 31st Int. Symp. Ind. Electron.*, 2022, pp. 200–205.

[19] K. Ohishi, K. Ohnishi, and K. Miyachi, "Torque-speed regulation of DC motor based on load torque estimation," in *Proc. IEEJ Int. Power Electron. Conf.*, 1983, pp. 1209–1216.

[20] T. Murakami and K. Ohnishi, "Observer-based motion control-application to robust control and parameter identification," in *Proc. Asia-Pacific Workshop Adv. Motion Control*, 1993, pp. 1–6.

[21] T. Uzunović and A. Šabanović, *Motion Control of Functionally Related Systems*. Boca Raton, FL, USA: CRC Press, 2020.

[22] T. Uzunović et al., "Combining real-time parameter identification and robust control algorithms for effective control of electrical machines," in *Proc. Int. Conf. Elect. Mach.*, 2022, pp. 2391–2396.

[23] T. Murakami, F. Yu, and K. Ohnishi, "Torque sensorless control in multidegree-of-freedom manipulator," *IEEE Trans. Ind. Electron.*, vol. 40, no. 2, pp. 259–265, Apr. 1993.

TARIK UZUNOVIĆ (Senior Member, IEEE) received the B.Eng. and M.Eng. degrees in electrical engineering from the University of Sarajevo, Sarajevo, Bosnia and Herzegovina, in 2008 and 2010, respectively, and the Ph.D. degree in mechatronics from Sabanci University, Istanbul, Turkey, in 2015.

He is currently an Associate Professor with the Department of Automatic Control and Electronics, Faculty of Electrical Engineering, University of Sarajevo. His research interests include control theory, motion control, robotics, and mechatronics.

ERAY A. BARAN received the B.Sc., M.Sc., and Ph.D. degrees in mechatronics engineering from Sabanci University, Istanbul, Turkey, in 2008, 2010, and 2014, respectively.
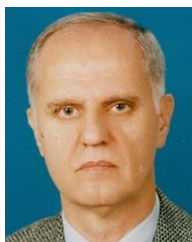
He is currently a Research Track Assistant Professor with the Department of Mechatronics Engineering and the Director of the Robotics and Intelligent Motion Control Laboratory, Istanbul Bilgi University, Istanbul, Turkey. His research interests include teleoperation systems, robust and intelligent motion control, robotics, and mechatronic systems.

İLKAY TURAÇ ÖZÇELIK received the B.S. degree in mechatronics engineering and the M.S. degree in electrical and electronics engineering from Istanbul Bilgi University, Istanbul, Turkey, in 2021 and 2023, respectively.

His research interests include motion control systems and bilateral control.

MINORU YOKOYAMA (Member, IEEE) received the B.E., M.E., and Ph.D. degrees in electrical and computer engineering from Yokohama National University, Yokohama, Japan, in 2015, 2017, and 2020, respectively.

Since 2020, he has been with the Institute of Technology, Tokyu Construction Company, Ltd., Kanagawa, Japan. His research interests include motion control, mechatronics, and haptics.

TOMOYUKI SHIMONO (Senior Member, IEEE) received the B.E. degree in mechanical engineering from Waseda University, Tokyo, Japan, in 2004, and the M.E. and Ph.D. degrees in integrated design engineering from Keio University, Yokohama, Japan, in 2006 and 2007, respectively.

From 2007 to 2008, he was a Research Fellow of the Japan Society for the Promotion of Science. From 2008 to 2009, he was a Research Associate with the Global Centers of Excellence Program, Keio University. Since 2009, he has been with the Faculty of Engineering, Yokohama National University, Yokohama, where he is currently an Associate Professor. His research interests include haptics, motion control, medical and rehabilitation robots, actuators, and sensors.

ASIF ŠABANOVIĆ (Life Senior Member, IEEE) received the B.S., M.S., and Dr.Eng. degrees in electrical engineering from the University of Sarajevo, Sarajevo, Bosnia and Herzegovina, in 1970, 1975, and 1979, respectively.

After graduation, he joined the Energoinvest-IRCA, Sarajevo. He is currently an Emeritus Professor and a Member of the Academy of Sciences and Arts of Bosnia and Herzegovina, Sarajevo. He was a Visiting Researcher with the Institute of Control Sciences, Moscow, Russia; a Visiting Professor with the California Institute of Technology, Pasadena, CA, USA; a Visiting Professor with Keio University, Yokohama, Japan; a Full Professor with Yamaguchi University, Ube, Japan; and the Head of the Department of Robotics, TÜBİTAK Marmara Research Center, Istanbul, Turkey. His research interests include control systems, motion control systems, robotics, mechatronics, and power electronics.